Article

The Microtubule-Based Cytoskeleton Is a Component of a Mechanical Signaling Pathway in Fly Campaniform Receptors

Xin Liang,[1] Johnson Madrid,[1] and Jonathon Howard[1,2,*]
[1]Max-Planck Institute of Molecular Cell Biology and Genetics, Dresden, Germany; and [2]Molecular Biophysics and Biochemistry, Yale University, New Haven, Connecticut

ABSTRACT In mechanoreceptors, mechanical stimulation by external forces leads to the rapid opening of transduction channels followed by an electrical response. Despite intensive studies in various model systems, the molecular pathway by which forces are transmitted to the transduction channels remains elusive. In fly campaniform mechanoreceptors, the mechanotransduction channels are gated by compressive forces conveyed via two rows of microtubules that are hypothesized to be mechanically reinforced by an intervening electron-dense material (EDM). In this study, we tested this hypothesis by studying a mutant fly in which the EDM was nearly absent, whereas the other ultrastructural elements in the mechanosensitive organelle were still present at 50% (or greater) of normal levels. We found that the mechanosensory response in this mutant was reduced by 90% and the sensitivity by at least 80%. To test whether loss of the EDM could lead to such a reduction in response, we performed a mechanical analysis and estimated that the loss of the EDM is expected to greatly decrease the overall rigidity, leading to a marked reduction in the gating force conveyed to the channel. We argue that this reduction in force, rather than the reduction in the number of transduction channels, is primarily responsible for the nearly complete loss of mechanosensory response observed in the mutant fly. Based on these experiments and analysis, we conclude that the microtubule-based cytoskeleton (i.e., microtubules and EDM) is an essential component of the mechanical signaling pathway in fly campaniform mechanoreceptor.

INTRODUCTION

External forces impinging on mechanoreceptors lead to the rapid opening of ion channels and ensuing electrical responses. The rapidity of mechanotransduction has led to the hypothesis that cellular structures provide a direct mechanical link to the transduction channels, without chemical intermediates whose diffusion would slow the response (1–4). These structures can be thought of as forming a mechanical signaling pathway. Despite efforts to determine the molecular basis of this mechanical signaling pathway in various model organisms (1–3,5), the details remain elusive.

We recently identified a set of seven serially linked structures in the distal tip of the dendrite of fly campaniform mechanoreceptors (6). The distal tip is thought to be the site of transduction in these cells (7,8). The structures are an extracellular sheath, sheath-membrane connectors (SMCs), the plasma membrane, the transduction channels, membrane-microtubule connectors (MMCs), microtubules (MTs), and an electron-dense material (EDM) (Fig. 1, *left*). The EDM in the middle of the distal tip is located between the two rows of microtubules, forming an MT-based cytoskeleton, which connects the structures on each side of the cell. In earlier work, a linkage model was proposed in which the compression of the distal tip, caused by cuticle deformation, leads to the transmission, through these structures, of compressive forces that act on and gate the transduction channels (Fig. 1, *right*) (6).

Because the structures are in series, the absence of any single element is predicted to break the pathway and thereby abolish the mechanosensory response. We previously reported that the MMCs are absent in *nompC* null mutants, which lack sensory responses (6). Although the lack of response could be due to a break in the mechanical linkage in the absence of MMCs, as predicted by the model, it is also possible that the loss occurs because NompC itself is likely the transduction channel (9–11). Therefore, further evidence is required to test the linkage model.

In this work, we examined a mutant strain (*f02655*) in which the EDM was nearly absent (12). We found that the mechanosensory response of this mutant strain was reduced by 90% and the sensitivity was reduced by at least 80%. However, only ~50% of the MTs, with their associated MMCs and possibly NompC channels, were missing. The other elements—the sheath, the SMCs, and the membranes—were present as in the wild-type flies. The large decrease in the sensory response is consistent with the EDM being a mechanical element in the linkage pathway.

Submitted June 23, 2014, and accepted for publication October 23, 2014.

*Correspondence: jonathon.howard@yale.edu

Johnson Madrid's present address is Institute of Biophysics, Johann Wolfgang Goethe University Frankfurt, Frankfurt am Main, Germany.

Editor: Alan Grodzinsky.

0006-3495/14/12/2767/8 $2.00

http://dx.doi.org/10.1016/j.bpj.2014.10.052

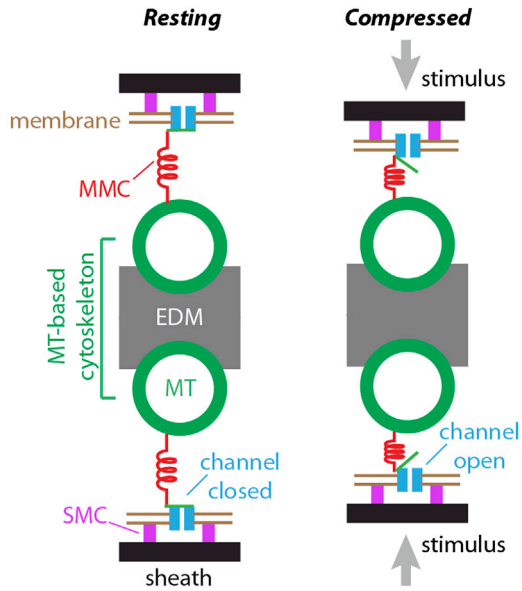

FIGURE 1 Model of the mechanical signaling pathway in the fly campaniform mechanoreceptor. (*Left*) A schematic of seven linked structures in the mechanoreceptive organelle of fly campaniform receptors (6). The MT and EDMs together are termed the MT-based cytoskeleton. (*Right*) The transduction channels are activated by the compressive force conveyed by the MTs via the MMCs. External forces are indicated by the gray arrows.

MATERIALS AND METHODS

Flies

All flies were maintained on standard medium at 23–25°C. *Oregon R* was used as the wild-type strain. The *f02655* strain (stock No. 18573) was from the Bloomington Stock Center (Bloomington, IN).

Electrophysiology recording and data analysis

Electrophysiology recording of the haltere campaniform receptors was performed as described previously (6). Briefly, a decapitated adult fly (2–3 days old) was immobilized by wax on a glass slide mounted on a ball-and-socket stage (M-RN-86, Newport, Irvine, CA). A tungsten electrode was placed near the haltere nerve. The reference electrode was inserted in the thorax. A sharp probe was mounted onto a piezo stack actuator (P216.90, Physikinstrumente, Germany), which was driven by a piezo amplifier/controller (E-481 PICA Piezo High-Power Amplifier/Controller, Physikinstrumente, Eschbach, Germany) to apply the mechanical stimuli to the pedicel campaniform receptor field of the haltere. We applied a square wave stimulation at 100 Hz. The voltage difference between the reference and recording electrodes was amplified with a differential amplifier (DAM50 Bio-Amplifier, WPI, Sarasota, FL). Labview was used to program the software to control the stimulation and record the signal. The data were sampled at 10 kHz and stored on computer.

Off-line data analysis was performed with MATLAB and IGOR Pro. The superimposition, averaging of 50 recording traces, and peak voltage detection were performed using MATLAB (Fig. 2, *B* and *D*). The distributions of the peak voltages shown in Fig. 2, *C* and *E*, were performed using IGOR Pro. The multipeak fitting shown in Fig. 2 *C* was calculated using the multipeak fitting package in IGOR Pro and the type of the peaks was chosen to be Gaussian. The single Gaussian peak fitting shown in Fig. 2 *E* was performed using IGOR Pro.

Transmission electron microscopy and image process

Transmission electron microscopy (TEM) was performed using the standard protocol as described previously (7). The TEM images were visualized using Fiji (13). The lengths of MMCs and the number of MTs in the TEM images were measured using Fiji.

Molecular biology

Total fly RNA was extracted with the RNeasy Kit (Qiagen, Venlo, The Netherlands). The cDNA was synthesized using SuperScript III Reverse Transcriptase (RT) (Life Technologies, Carlsbad, CA). All polymerase chain reactions (PCRs) were performed with Phusion DNA polymerase (New England Biolabs, Ipswich, MA). The PCR products were cloned into pGEMT vector (Promega, Madison, WI) and sequenced using standard procedures (DNA sequencing facility, MPI-CBG, Dresden, Germany).

Antibody generation, Western blot, and immunostaining

The procedure of antigen and antibody screening was performed using standard procedures (Antibody facility, MPI-CBG) and has been described previously (7). The antigen chosen to generate the antibody was a fragment of 204 amino acids in DCX-EMAP sequence (amino acids 258–461). The positive clones were finally tested on human embryonic kidney (HEK) 293FT cells transiently transfected with C-terminal green-fluorescent-protein (GFP)-tagged full-length DCX-EMAP by immunostaining and Western blot (Fig. S1 in the Supporting Material). The DCX-EMAP-GFP was made by cloning full-length DCX-EMAP into pcDNA3.1/CT-GFP-TOPO (Life Technologies) and transfected into HEK 293FT cells by Fugene HD reagent (Roche, Germany).

Western blot and immunostaining of the cells and tissues were performed as described previously (7). The number of the clone used for the tissue staining shown in Fig. 3 and Fig. S1 was 1357-E08. The α-tubulin antibody used was from Abcam (ab15246; Cambridge, United Kingdom).

RESULTS AND DISCUSSION

The *f02655* mutation strongly reduces the sensory response of campaniform receptors

In earlier work using DNA arrays, we found that the gene for DCX-EMAP, a member of the EMAP family (echinoderm-MT-associated proteins) that contains two doublecortin domains, was preferentially expressed in the campaniform mechanoreceptors in the fly haltere (12). Adult flies carrying a *piggyBac* insertion in the *dcx-emap* gene (*f02655* strain) were deaf, as judged by the lack of electrical responses to mechanical stimulation of Johnston's organ, the fly's auditory organ. The loss of auditory transduction shows that DCX-EMAP is essential for transduction by chordotonal-type mechanoreceptors that mediate hearing in flies (12).

The *f02655* mutant flies were also uncoordinated, as shown by a flight test (12), suggesting a possible disruption in transduction mediated by campaniform mechanoreceptors. Campaniform receptors belong to a nonchordotonal class of ciliated fly mechanosensory cells that also includes bristle receptors. Campaniform receptors respond

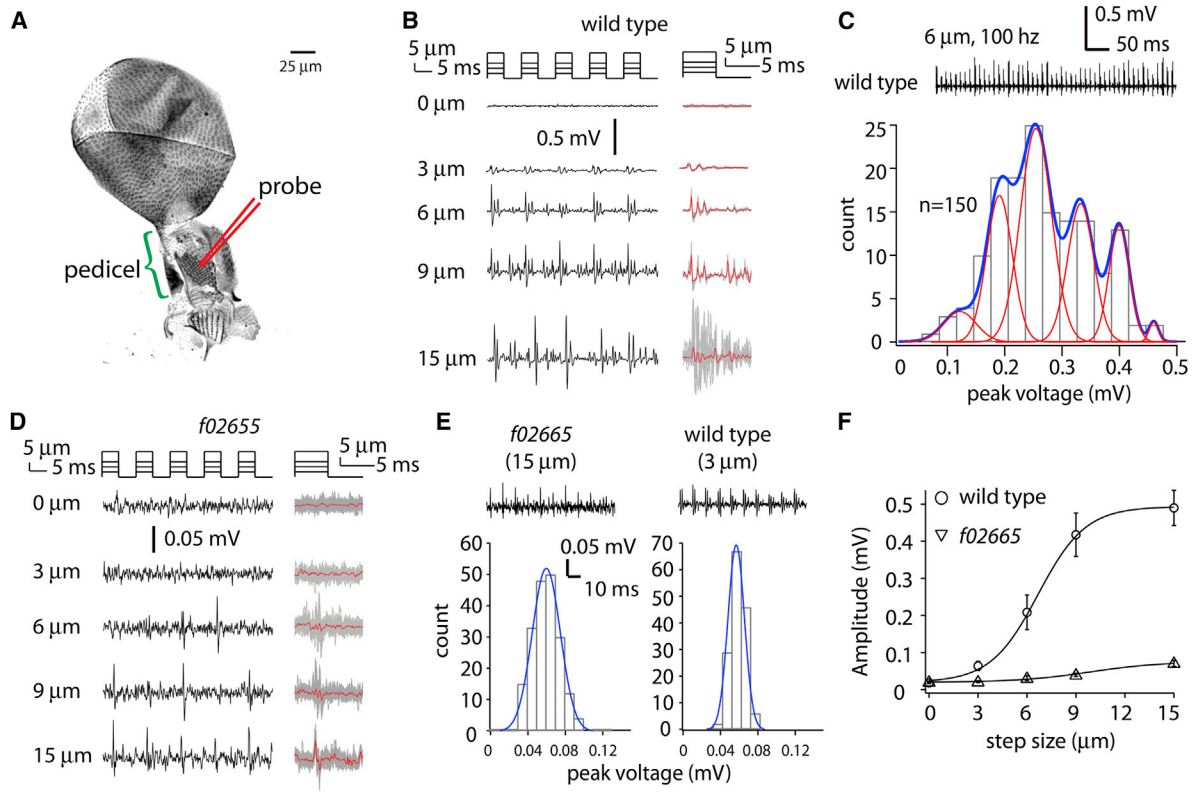

FIGURE 2 Electrophysiological responses of campaniform mechanoreceptors in wild-type and mutant flies. (*A*) An image of a fly haltere. The mechanical probe (*red*) was positioned in the middle of the receptor field in the pedicel (*green bracket*). The cuticular structures that overlay the campaniform receptors are visible in the pedicel. This image of the haltere is used to indicate the position of the stimulation probe; the actual recording was performed on intact living flies immobilized on the stage. (*B*) Representative recording traces from a wild-type fly in response to different mechanical stimuli (*uppermost curves*). Typical response traces to five cycles of stimulation are shown at left. At right, the responses to 50 cycles are aligned with the stimulation cycles and overlaid (*gray*). The average trace is also shown (*red*). Note that the individual responses to 15-μm stimuli lose synchronicity with the stimulation (the gray lines do not overlap with each other as they do for 3- to 9-μm stimuli). (*C*) The distribution of the peak response amplitudes to 150 6-μm stimuli. An example of a response to 50 stimuli is shown above. The broad distribution of response amplitudes can be fit with a multipeaked distribution. (*D*) Representative recording traces from a mutant fly in response to different mechanical stimuli (note that the scale of the response traces differs from that in *B*). Typical recording traces of five cycles are shown at left. At right, the responses to 50 cycles are overlaid (*gray*) and the average trace is shown (*red*). (*E*) The distribution of the amplitudes of responses to 15-μm stimuli in a mutant receptor was similar to that to 3-μm stimuli in a wild-type receptor. The histograms have single peaks at $P_{f02655} = 0.060$ mV and $P_{WT} = 0.057$ mV. The representative recording traces for 100 ms (10 cycles) are shown above the histograms. Note that wild-type receptors showed multiple spikes, whereas mutant receptors showed only a single spike. (*F*) The average peak response amplitudes from campaniform receptors in *f02655* mutant flies (*triangles*) were significantly smaller than those in wild-type flies (*circles*). Data are represented as the mean $\pm$ SE ($n = 4$–6 flies/data point).

to deformations of the cuticle and are especially prominent in the halteres, which function as gyroscopes to stabilize flight (14).

To determine whether the *f02655* mutation affects campaniform receptors, we measured mechanically evoked electrophysiological responses using an extracellular recording setup (6). Briefly, a recording tungsten electrode was inserted into an immobilized fly at the base of the haltere near the haltere nerve. A reference electrode was inserted in the thorax. A sharp probe mounted to a piezo stack actuator was used to mechanically stimulate the campaniform receptor field on the dorsal side of the haltere pedicel (Fig. 2 *A*).

In wild-type flies, the minimal stimulus with which we could record a consistent electrical response was 3 μm (Fig. 2 *B*). The average of the peak voltage of each response to the 3-μm stimulus was 0.064 $\pm$ 0.012 mV. With 6-μm and 9-μm stimuli, the average peak voltage increased to 0.21 $\pm$ 0.04 mV and 0.42 $\pm$ 0.06 mV, respectively. By aligning the individual response traces, we noted that the responses to 3- to 9-μm stimuli were synchronized with the stimulus: the temporal patterns of the spikes were similar in all stimulation cycles (Fig. 2 *B*). With the 15-μm stimuli, the average peak voltage was 0.49 $\pm$ 0.05 mV. Unlike the response to smaller stimuli, however, the individual responses to 15-μm stimuli became desynchronized with the stimulus: the temporal patterns of the spikes were different in each stimulation cycle, so that the averaged response actually decreased (Fig. 2 *B*), even though the amount of activity (Fig. 2 *B*, *right column*, *gray curves*) and the average

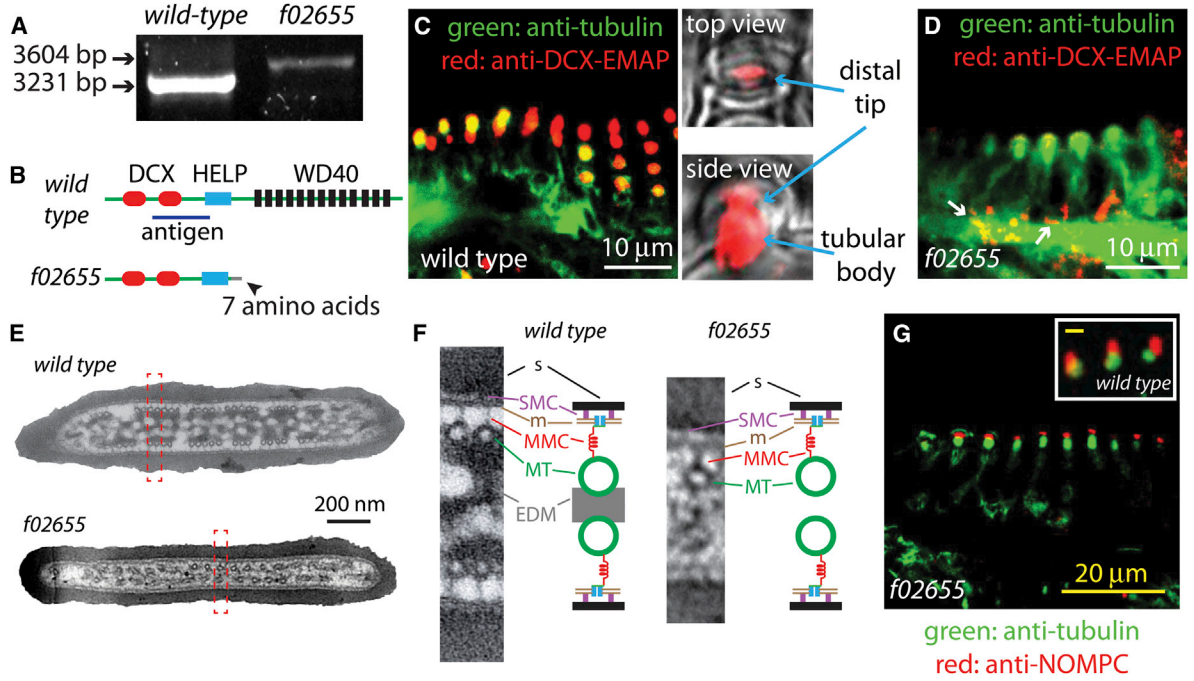

FIGURE 3 Characterization of the *f02655* strain. (*A*) The wild-type (*left lane*) and *f02655* mutant (*right lane*) transcripts of *dcx-emap* gene were amplified using RT-PCR. A longer transcript (3604 bp) was detected in the *f02655* strain. Note that in the *f02655* sample, no wild-type transcript was detected. (*B*) Protein domain organization in the wild-type (*upper*) and *f02655* mutant DCX-EMAP (*lower*). The additional sequence from the *piggyBAC* insertion was predicted to introduce seven amino acids (*black arrowhead*) after cysteine 532 in the DCX-EMAP protein sequence. An in-frame stop codon after the sequence coding the seven amino acids was predicted to lead to the prematuration of the DCX-EMAP protein, which would only contain the doublecortin and HELP domains, but not the WD40 domain (*lower*). The blue line (*upper*) indicates the fragment of DCX-EMAP (amino acids 258–461, 204 amino acids) used as the antigen to generate the DCX-EMAP antibody. (*C*) In the campaniform mechanoreceptors of the wild-type flies, the DCX-EMAP antibody specifically stained the distal part of the dendrites (*left*), including the distal tip (*upper right*) and the tubular body (*lower right*). The campaniform mechanoreceptors shown at lower right are located in the pedicel of a wild-type haltere (Fig. 2 *A*). (*D*) In the *f02655* strain, the immunofluorescence signal of DCX-EMAP was absent in the distal tips and tubular bodies of the campaniform mechanoreceptors. Some residual signals were observed in some cells (*white arrows*). Note that the tubulin signal was overexposed to visualize the tubular bodies of the campaniform receptors. The campaniform mechanoreceptors shown are located in the pedicel of an *f02655* mutant haltere. (*E*) The ultrastructure of the distal-tip region in cross section in wild-type (upper *panel*) and *f02655* mutant cells (*lower*). (*F*) Magnified images of the cross sections outlined in red in *E* and their corresponding schematics indicate that there are ultrastructural differences between wild-type cells (*left*) and mutant cells (*right*). The EDM was nearly absent in the mutant cells (*lower left*), whereas the other structural elements were present. Abbreviations: s, sheath; SMC, sheath membrane connector; m, membrane; MMC, membrane MT connector; MT, microtubule; EDM, electron dense material. (*G*) NompC (*red*) localization in the campaniform receptors (*green*) of the *f02655* strain. (*Inset*) NompC localization in the wild-type campaniform receptors. Note that only the distal parts of the campaniform receptors are shown. Scale bar, 2 μm.

of the peak response of individual traces both increased. We could not apply reproducible stimuli >15 μm because larger deflections lead to slipping of the probe along the curved haltere surface.

The electrical responses are compound action potentials from a group of campaniform receptors stimulated by the probe. This interpretation is based on the following evidence:

1. Earlier work showed that the responses are normal in the *atonal* mutant, which abolished responses in chordotonal receptors (6). Thus, the response originates from the campaniform receptors rather than from chordotonal organs in the haltere.
2. It is unlikely that only one receptor would be activated at a time by our mechanical probe. The campaniform receptors in the field are closely packed one next to the other (see pedicel receptor field in Fig. 2 *A*; also see Liang et al. (7)). Our mechanical probe was positioned in the middle of the receptor field (Fig. 2 *A*), and the tip diameter (~5 μm) was larger than the size of the cuticle cap overlaying one receptor. Therefore, the probe was likely to stimulate more than one receptor.
3. The response was recorded from the haltere nerve, and no graded signals from individual neurons (i.e., local receptor potentials) were expected. Rather, the observation of an increasing response with increasing stimulus intensity is likely due to activation of more receptors.
4. When the individual responses to 3- to 9-μm stimuli were aligned, we noticed that the shapes of the individual responses in different stimulation cycles were similar, but their amplitudes often varied considerably from one stimulus to the next (Fig. 2 *B*); for example, at 6-μm stimulus, the peak response varied fivefold,

from 0.1 mV to 0.5 mV (Fig. 2 *C*). A simple explanation for this variation is that the response was the superposition of a number of responses from different receptors that were activated stochastically in each stimulus cycle. Consistent with this explanation, we found that the histogram of peak responses to 6-μm stimuli could be fit to a multipeak distribution (Fig. 2 *C*) with a distance between adjacent peaks of 0.067 $\pm$ 0.007 mV (mean $\pm$ SD, $n = 5$). This distance is close to the average amplitude of the minimal responses that we recorded with the 3-μm stimulus (0.064 mV; see Fig. 2 *E*, *right*). This suggests that the elementary event resolved in our recording experiments is likely a spike from a single neuron or a set of neurons and that the total response to larger stimuli is due to activation of several neurons.

5. The responses in a single cycle often contained several spikes of different peak voltage (for example, see the 6-μm and 9-μm traces in Fig. 2 *B*), further suggesting that the responses were from more than one receptor.

Therefore, we conclude that in wild-type flies, the electrical signal is a compound response from a group of campaniform receptors and that the peak amplitude reflects the number of receptors that are simultaneously activated by each stimulus.

The electrical responses in the *f02655* strain were greatly attenuated (Fig. 2 *D*; note that the scale is different from that in Fig. 2 *B*). With 3-μm stimuli, no response was detected. With 6- and 9-μm stimuli, small responses were detected only in some cycles. With 15 μm stimuli, the amplitude was 0.070 $\pm$ 0.005 mV (Fig. 2 *D*), comparable to wild-type flies in response to 3-μm stimuli. The individual responses to 15-μm stimuli were of stereotyped amplitude, with the distribution of amplitudes showing only a single peak (Fig. 2 *E*, *left*), like wild-type responses to 3-μm stimuli (Fig. 2 *E*, *right*) and different from wild-type responses to 6- and 9-μm stimuli (Fig. 2 *C*). The wild-type responses to 3-μm stimuli, however, were more vigorous than the mutant responses to 15-μm stimuli, as the former always showed multiple spikes, whereas the latter showed only a single spike (Fig. 2 *E*).

We measured the average of the peak voltage of individual responses to 50 stimulus cycles (10 ms/cycle, 0.5 s in total) in wild-type and *f02655* mutant flies. For each stimulus, data from four to six flies were used for statistical analysis (Fig. 2 *F*). The average response in the *f02655* strain was much weaker than that in wild-type flies (Fig. 2 *F*). For example, the magnitude of response to 6-μm and 9-μm stimulation in the *f02655* strain (after background subtraction) was ~10% and ~8%, respectively, of that in wild-type flies. Based on the different response amplitudes to the same stimulus levels, and on the different stimulus levels required to give the same response, we conclude that the *f02655* mutation leads to a reduction in response by up to 90% and a decrease in sensitivity by >80%.

The *f02655* mutation has a mild ultrastructural phenotype

To determine the molecular and cellular origin of the reduction in mechanosensory sensitivity, we performed a molecular and ultrastructural analysis. The *f02655* strain has a *piggyBAC* insertion in the *dcx-emap* gene, leading to a longer transcript (Fig. 3 *A*). We sequenced this mutant transcript and compared it with the wild-type transcript. Both transcripts were spliced. The longer transcript in the mutant was due to mis-splicing and insertion of part of the *piggyBAC* sequence into the mRNA (compared with the *piggyBAC* construct sequence (GenBank accession no. AY515148)). No wild-type transcripts were detected in the *f02655* sample, suggesting that the *piggyBAC* insertion efficiently disrupted the splicing of the *dcx-emap* gene at the mRNA level. Due to an in-frame stop codon in the *piggyBAC* sequence, the mRNA in the mutant was predicted to produce a truncated protein containing only the doublecortin domain, the HELP domain, and an additional seven amino acids from the *piggyBAC* sequence (after cysteine 532 in the DCX-EMAP sequence) (Fig. 3 *B*).

To examine whether the DCX-EMAP protein level was reduced in the mutant, we generated a monoclonal antibody against a fragment of the DCX-EMAP protein that is also present in the predicted truncated protein in the mutant (Fig. 3 *B*). The antibody was tested using the full-length DCX-EMAP expressed in HEK293 cells. The antibody specifically stained the transfected cells (Fig. S1 *A*, *upper right*), and the signal colocalized with the GFP signal (Fig. S1 *A*, *lower left*). The antibody detected the DCX-EMAP-GFP protein expressed in the HEK293 cells by Western blot (Fig. S1 *B*). These two experiments show that the antibody preferentially recognizes DCX-EMAP.

Using the antibody, we found that DCX-EMAP was localized to the distal end of the dendrite in the campaniform mechanoreceptor (Fig. 3 *C*, *left*), consistent with the previous study using overexpression of a tagged protein (12). Specifically, we found that DCX-EMAP localized to both the distal tip (Fig. 3 *C*, *upper right*) and the tubular body (Fig. 3 *C*, *lower right*). These two regions both contained MT-based cytoskeletal structures (7). Therefore, the endogenous localization of DCX-EMAP in fly campaniform mechanoreceptors was consistent with its predicted function as an MT-associated protein (12). In the *f02655* strain, antibody staining indicated that the amount of DCX-EMAP was nearly absent in the distal tips and the tubular bodies of the campaniform receptors (Fig. 3 *D*). A weak signal in the cell body (Fig. 3 *D*, *arrows*) may indicate a small residual amount of the truncated protein, which is predicted to be recognized by the antibody (Fig. 3 *B*). With the RT-PCR

and immunostaining experiments, we conclude that the amount of transcripts and protein products of the *dcx-emap* gene in the *f02655* mutant is negligible.

The most prominent ultrastructural phenotype of the *f02655* strain is the near absence of EDM in the distal tips of the mutant cells (Fig. 3 *E*, *lower*). Thus, DCX-EMAP is necessary for the assembly or maintenance of the EDM. Despite the ultrastructural changes in the central region of the distal tip, the number of MTs in the mutant cells is reduced by only ~50% (wild-type, 46 ± 7 MTs (mean ± SD), $n = 8$ cells; *f02655*, 23 ± 7 MTs, $n = 5$ cells) (Fig. 3 *E*). Another difference is that the MTs in the mutant cells are not clustered into small arrays as they are in wild-type cells (Fig. 3 *E*). The MMCs are present (Fig. 3 *F*) at an MMC/MT ratio of 0.75 in the *f02655* strain, close to the MMC/MT ratio in wild-type cells (0.80) (6). As the number of MTs was reduced by one-half, so too was the number of MMCs. The length of MMCs in mutant cells was 18.1 ± 4.2 nm ($n = 86$ MMCs, mean ± SD), the same as in wild-type cells (6). The other ultrastructural elements, including the sheath, the SMCs, and the plasma membrane, were present and appeared normal (Fig. 3 *F*).

Because NompC is a candidate subunit of the mechanotransduction channel (10), we further checked its expression in the *f02655* strain. We found that the expression of NompC was normal and we did not see a significant reduction in the NompC antibody signal in mutant receptors compared to wild-type receptors (Fig. 3 *G*). In mutant receptors, the NompC antibody signal exclusively localized in the distal tip of the mutant cells (Fig. 3 *G*), as in the wild-type cells (Fig. 3 *G*, *inset*) (7), suggesting that there is no mislocalization of NompC or accumulation of NompC elsewhere in the cells. The actual number of NompC molecules in the distal tip of mutant cells could not be quantified from the antibody staining. However, given that the ankyrin-repeat domain of NompC likely contributes to the MMCs (6) and that there are still ~50% MMCs remaining in the *f02655* strain, we estimate that there are at least 50% of the NompC molecules in the distal tip (perhaps >50% if the NompC molecules are not tethered to the MTs). We conclude that although the *f02655* strain is missing the EDM, the other elements in the putative mechanical signaling pathway are still present at 50–100% of normal levels.

The MT cytoskeleton has structural and mechanical roles in mechanotransduction

Our experimental data show that in the *dcx-emap* mutant, the electron-dense material is nearly absent and the MT-based cytoskeleton is disrupted. Other structural components in the distal-tip region of the campaniform receptor are approximately normal (50–100% of the wild-type level). In contrast to this intermediate structural phenotype, the haltere campaniform receptors in this mutant lost nearly all their mechanosensory response (90% reduction in response). Based on these results, we now discuss two possible ways that the MT-based cytoskeleton contributes to the functional defects in the *f02655* strain.

First, the reduction in response may be partly due to a reduction in the number of transduction channels. The density of MMCs in the distal-tip region is high, ~650 MMCs/μm^2 of the plasma membrane. In our previous work, we have shown that the MMCs are dependent on the presence of NompC channels and are likely composed of the ankyrin-repeat domain of NompC. This density of MMCs (i.e., NOMPC channels) is intermediate between the estimated density of the voltage-sensitive ion channels in the axon initial segment (100–200 channels/μm^2) (15) and the channel density at the nodes of Ranvier along the axons (1000–2000 channels/μm^2) (15). The high channel densities at the axon initial segment and the nodes of Ranvier are achieved though membrane-cytoskeleton-associated proteins (e.g., ankyrin). We note that it is similar in the fly campaniform receptors: the NompC channels are also linked to the cytoskeleton through their ankyrin-repeat domain. When the EDM was absent and the number of MTs was reduced in the *f02655* strain, we observed a reduction in the number of MMCs and estimated up to 50% loss of the NompC channels, suggesting that MTs may play a role in maintaining such a high density of MMCs and NompC channels in the distal-tip region. In wild-type flies, the clustering of NompC channels at such a high density is expected to ensure the mechanosensitivity of campaniform mechanoreceptors to stimulation (e.g., deformation of the cuticle on the nanometer scale) and to keep the capability of cells to generate an adequate receptor potential to initiate the action potential. Therefore, a reduction in the number of transduction channels in the *f02655* strain is expected to contribute to the decrease of the compound action potential, as we observed in the electrophysiology experiments.

However, we do not think that a 50% reduction in channel number (up to 50%) is sufficient to account for the 90% decrease in response. This is based on two arguments. First, the response threshold in the mutant is ~6 μm, yet when the stimulus is reduced twofold to 3 μm in the wild-type, the response is still well above threshold, as indicated by the observation of multiple spikes (Fig. 2 *B*). Thus, a simple doubling of the stimulus amplitude cannot compensate for a 50% decrease in channel number. And second, when the stimulus is increased fivefold, the response in the mutant to a 15-μm stimulus is still weaker than the response in the wild-type to a 3-μm stimulus. Thus, the sensitivity is reduced fivefold, much larger than a twofold decrease in channel number. Therefore, we think it is likely that in addition to the reduction in channel number, there is a reduction in the transmission of force from the stimulus to the channels due to the disruption of the MT-based cytoskeleton structure.

To examine the possibility that the disruption of MT-based cytoskeleton contributes to the reduction in response sensitivity by causing a reduction of force transmission to the channels, we performed a mechanical analysis.

First, we considered a simple mechanical model for transduction (Fig. 4 *A*). We assumed that deformations of the cuticle lead to a compressive deformation, D, of the distal tip, which in turn, through the compliance of the links (C_t), leads to a force

$$F_g = \frac{D}{C_t}$$

acting on each channel (Fig. 4 *A*). In this model, we assume that there is one channel per MMC and one MMC per MT (see Liang et al. (6) for the detailed ultrastructure). If opening of the channel is associated with a displacement, d, of the attachment point of the MMC to the channel (Fig. 4 *A*) in the direction of this force, then the open/closed probability ratio will increase by a factor of

$$\exp\left(-F_g d/kT\right),$$

where k is the Boltzmann constant and T is the absolute temperature. Because the cuticle is very rigid, we assume that the compressive displacement, D, does not depend on the compliance of the links (C_t). According to this model, the gating force depends inversely on the compliance, so a larger compliance will lead to lower sensitivity.

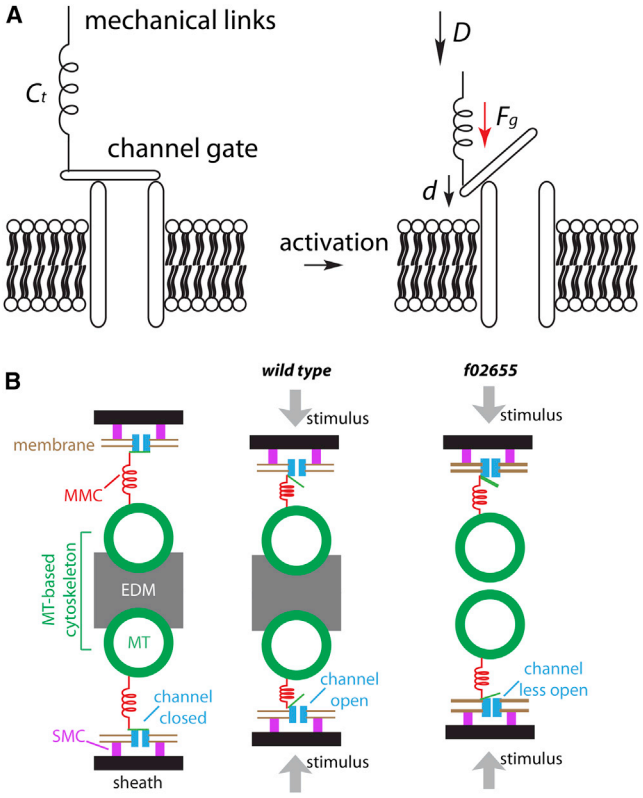

FIGURE 4 Mechanical analysis. (*A*) A simple mechanical gating model showed that the transduction channel and the mechanical links (C_t) are connected in series (*left*). In response to the compression stimulus, D, a gating force (F_g) is generated to deflect the channel gate (d), which leads to the opening of the channel. (*B*) In wild-type cells, the EDM prevents the MTs from approaching each other (*left*), so most of the deformation D is taken up by the MMCs and the membrane (*middle*). In *f02655* mutant cells, the absence of the EDM allows the two rows of MTs to move toward each other, thereby taking up some of the deformation, D. The additional displacement of the MTs increases the compliance of the links, which would lead to a smaller gating force and a weaker electrical response.

Because the links are in series, the compliance of the whole pathway is the sum of the compliances of the individual elements. On structural grounds, the sheath, SMC, MTs, and EDM are expected to be much stiffer (i.e., less compliant) than the MMCs, which are long, thin filaments. Thus, in the wild-type cells (Fig. 4 *B*), C_t is primarily due to the compliance of the MMCs and the membrane. These compliances are estimated to be 0.25 nm/pN (MMC) and 0.17 nm/pN (membrane) per channel (see Liang et al. (6)), so the total compliance of the wild-type cell is 0.42 nm/pN per channel. We expect that the EDM reinforces the two rows of MTs by preventing them from approaching each other (thereby taking up some of the total deformation, D) (Fig. 4 *B*). In the *f02655* mutant receptor, the EDM is significantly reduced, so this support will be absent (Fig. 4 *C*). This could lead to a very large compliance, effectively short-circuiting transduction and leading to a nearly complete loss of the electrical response, as observed. We conclude that the MT-based cytoskeleton (i.e., the MTs and the EDM) provides mechanical rigidity to convey force to the transduction channels. The loss of this support would lead to the decrease in the force transmission to the channels and in turn to the reduction in sensory response.

Why is there a residual response in the mutant (~10%)? One possibility is that the MTs themselves are rigid enough to provide an EDM-independent stiffness so that the channels can be partially activated. This could occur if the MTs are anchored at one or both ends (e.g., if at the proximal end they emerge from the tubular body, or at the distal end they terminate at the most peripheral part of the cell). We estimate the compliance of the remaining individual MTs with the help of the beam equation (16):

$$C_{mt} = \frac{L^3}{3EI},$$

where L is the length from one of the ends, which is assumed to be clamped (it cannot pivot) and EI is the flexural rigidity of the MT. Assuming that $L = 0.3\ \mu$m, half the length of the distal tip, and $EI = 24 \times 10^{-24}\ \mathrm{N \cdot m^2}$ (16), then the compliance is ~0.4 nm/pN. Our estimate of this compliance is only approximate: if the ends are not held firmly, the compliance

will be greater, whereas if the MTs are clamped at both ends, then the compliance will be less. This value of the compliance is similar to that of the MMC-membrane combination, suggesting that the individual MTs are not rigid enough to mechanically support force transmission as in the wild-type flies, but it may explain the residual stiffness responsible for the non-zero sensitivity in the mutant receptors. Conversely, the relatively high compliance of the MTs suggests that mechanical reinforcement by the EDM is necessary so that force can be conveyed to the channels via the MMCs.

SUMMARY

Our observations on the *f02655* mutant support the idea that signal transduction in campaniform reception contains a mechanical signaling pathway that couples external forces to the transduction channels. Such a mechanical signaling pathway serves two purposes. First, direct linkage is faster than indirect linkage via diffusion of a chemical intermediate. And second, the compliance of the signaling pathway can provide a match between the impedance of the cuticle, which is high, to that of the channels, which is low, ensuring that the large forces acting on the cuticle do not overwhelm the channel's gating mechanism.

SUPPORTING MATERIAL

One figure and it's legend is available at http://www.biophysj.org/biophysj/supplemental/S0006-3495(14)00140-0.

The authors thank Heike Petzold and Antje Franz for the general lab organization and Joshua Alper, Fernando Carrillo and Mohammed Mahamdeh for their helpful comments on the manuscript. Special thanks to the protein expression facility, antibody facility, electron microscopy facility, and light microscopy facility at MPI-CBG for their technical support.

We acknowledge funding for this study from the Max-Planck Society.

REFERENCES

1. Lumpkin, E. A., K. L. Marshall, and A. M. Nelson. 2010. The cell biology of touch. *J. Cell Biol.* 191:237–248.
2. Gillespie, P. G., and U. Müller. 2009. Mechanotransduction by hair cells: models, molecules, and mechanisms. *Cell.* 139:33–44.
3. Gillespie, P. G., and R. G. Walker. 2001. Molecular basis of mechanosensory transduction. *Nature.* 413:194–202.
4. Corey, D. P., and A. J. Hudspeth. 1983. Kinetics of the receptor current in bullfrog saccular hair cells. *J. Neurosci.* 3:962–976.
5. Delmas, P., and B. Coste. 2013. Mechano-gated ion channels in sensory systems. *Cell.* 155:278–284.
6. Liang, X., J. Madrid, …, J. Howard. 2013. A NOMPC-dependent membrane-microtubule connector is a candidate for the gating spring in fly mechanoreceptors. *Curr. Biol.* 23:755–763.
7. Liang, X., J. Madrid, …, J. Howard. 2011. NOMPC, a member of the TRP channel family, localizes to the tubular body and distal cilium of *Drosophila* campaniform and chordotonal receptor cells. *Cytoskeleton* (*Hoboken*). 68:1–7.
8. Keil, T. A. 1997. Functional morphology of insect mechanoreceptors. *Microsc. Res. Tech.* 39:506–531.
9. Walker, R. G., A. T. Willingham, and C. S. Zuker. 2000. A *Drosophila* mechanosensory transduction channel. *Science.* 287:2229–2234.
10. Yan, Z., W. Zhang, …, Y. N. Jan. 2013. *Drosophila* NOMPC is a mechanotransduction channel subunit for gentle-touch sensation. *Nature.* 493:221–225.
11. Effertz, T., B. Nadrowski, …, M. C. Göpfert. 2012. Direct gating and mechanical integrity of Drosophila auditory transducers require TRPN1. *Nat Neurosci.* 15:1198–1200.
12. Bechstedt, S., J. T. Albert, …, J. Howard. 2010. A doublecortin containing microtubule-associated protein is implicated in mechanotransduction in *Drosophila* sensory cilia. *Nat. Commun.* 1:11.
13. Schindelin, J., I. Arganda-Carreras, …, A. Cardona. 2012. Fiji: an open-source platform for biological-image analysis. *Nat. Methods.* 9:676–682.
14. Pringle, J. W. S. 1948. The gyroscopic mechanism of the halteres of Diptera. *Philos. Trans. R. Soc. Lond. B Biol. Sci.* 233:347–384.
15. Safronov, B. V., M. Wolff, and W. Vogel. 1999. Axonal expression of sodium channels in rat spinal neurones during postnatal development. *J. Physiol.* 514:729–734.
16. Howard, J. 2001. Mechanics of Motor Proteins and the Cytoskeleton. Sinauer Associates, Sunderland, MA.